Startup of a reactive distillation process with a decanter

F. Forner [a], M. Brehelin [b], D. Rouzineau [b], M. Meyer [b], J.-U. Repke [a,*]

[a] *Institute of Process and Plant Technologies, Technische Universität Berlin, KWT-9, Strasse des 17. Juni 135, 10623 Berlin, Germany*
[b] *ENSIACET/Laboratoire de Génie Chimique, 5 rue Paulin Talabot, 31106 Toulouse, France*

Abstract

The startup of a reactive distillation process for the production of propyl acetate including a decanter is studied. A simulation model is presented which describes the whole startup from a cold and empty state and takes into account the liquid phase split in the decanter. The simulation model is successfully validated with own dynamic experimental data. Different startup strategies are developed and analysed in simulation studies showing the high influence of the initial charging of decanter and reboiler on the startup time.

Keywords: Reactive distillation; Startup; Dynamic simulation; Experimental validation

1. Introduction

Reactive distillation (RD) is a favourable process alternative for esterification reactions, since these are limited by chemical equilibrium and the systems usually show azeotropic behaviour. The successful commercialization of a RD process for the synthesis of the high-volume product methyl acetate by esterification (proposed by Agreda and Partin [1]) has led to intensified research on RD. An overview of industrial RD applications is presented in Ref. [2]. Tang et al. [3] have recently compared different process designs for the esterification of acetic acid with C1–C5 alcohols. For esterification systems with ethanol or higher alcohols, the occurrence of large miscibility gaps can be exploited for the separation by integrating a decanter in the process. The experimental and theoretical studies of the esterification of butanol and acetic acid carried out by Singh et al. [4] show the potential of such a RD process to produce high-purity butyl acetate. Khaledi and Bishnoi [5] developed a simulation model for three-phase RD which takes into account the possible formation of two liquid phases not only in the decanter but in the whole column. Different processes are analysed showing that for the considered esterifications (butyl acetate and hexyl acetate production) formation of two liquid phases only occurs in the condenser-decanter unit and not inside the RD column.

* Corresponding author. Tel.: +49 30 31422486; fax: +49 30 31426915.
E-mail address: jens-uwe.repke@tu-berlin.de (J.-U. Repke).

In this contribution the esterification of acetic acid (HOAc) with *n*-propanol (PrOH) forming *n*-propyl acetate (PrOAc) and water (H_2O) as shown in Eq. (1) is studied. In our previous paper [6], reaction kinetics have been modelled and the feasibility and conceptual design of such a process has been shown by simulation and pilot plant experiments:

$$\mathrm{PrOH} + \mathrm{HOAc} \rightleftharpoons \mathrm{PrOAc} + \mathrm{H_2O} \quad (1)$$

In the present contribution, the startup of this RD process including a decanter is studied. In general, the startup of a distillation column is the transition from a cold and empty state to the desired operating point. It represents the most complex dynamic procedure in column operation so that the process knowledge gained in this contribution can be applied to other issues such as disturbance behaviour or product switch-over. Reducing startup time is an important task since during startup the products do not meet the specifications and this period is therefore very cost-intensive. Different startup strategies can be applied to reach the operating point. In conventional startup the manipulated variables (reflux ratio, reboiler duty, feed specifications) are always at the set point values without any manipulation. Alternative startup strategies for non-reactive distillation have been proposed using total reflux [7], total distillate removal [8] or optimised values for manipulated variables [9] during a certain period of time. Tran [10] has studied non-reactive three-phase distillation in a tray column with a decanter. He has shown both by experiment and simulation that the startup time depends strongly on

the composition of the initial holdup in the decanter. Surprisingly, for ethanol/water/cyclohexane, a system with multiple steady states, initial charging of ethanol (bottom product) to the decanter led to a reduction of about 60% of startup time. On the other hand charging a two-phase mixture close to steady-state composition extended the startup time. Different steady states could be reached with different startup strategies. The interactions between separation and reaction renders the process dynamics even more complex so that special strategies are needed for the startup of RD. For the startup of two-phase homogeneously catalyzed RD in tray columns Reepmeyer et al. [11] have shown that initial charging of the column trays with product can lead to a significant reduction of startup time. This strategy can only be applied to tray columns since it is practically not possible to initially charge a packed column with a significant liquid holdup. Forner et al. [12] emphasize this difference between packed and tray columns. They study the startup of RD for the methyl acetate synthesis in a tray and a packed column. As an alternative startup strategy for the packed column they consider initial charging of the reboiler and the distillate drum. Scenna et al. [13] and Scenna und Benz [14] focus on the influence of initial charging on avoiding undesired operating points for RD processes showing multiple steady states. Wu et al. [15] simulate the startup of a RD process for ethyl acetate production and find a strong dependence of startup time on condenser liquid holdup. First studies of the startup of a RD process for the production of propyl acetate with a decanter including a model validation have been presented in our previous publication [6]. In the present paper the developed startup model for the RD process including the decanter is presented in detail together with the experimental validation. Results from the analysis of two different process designs are shown. The influence of initial charging of decanter and reboiler with different compositions is studied.

2. Modelling and simulation

For the modelling of reactive distillation in packed columns, both equilibrium stage (EQ) and non-equilibrium stage (NEQ) approaches are used [16]. For esterification processes the simpler EQ models have shown good results in comparison with stationary experimental data [17–19]. During the startup of a distillation column the hydraulic variables (flow rates, holdups) and thermodynamic variables (temperatures) undergo large changes [20]. Due to these transitions it is not possible to describe the whole startup from a cold and empty state to the operating point with the typical EQ model. Different sets of equations are needed for the different distinguishable phases of the startup, requiring a switching between these model equations at certain points. In the course of this procedure the special startup model evolves into the dynamic EQ model for the operating range. This approach which is implemented in gPROMS® has been validated for the startup of two-phase RD in tray columns by Reepmeyer et al. [11] and for two-phase RD in columns with structured packing by Forner et al. [12]. In the present paper the model is used to describe RD in a randomly packed column and is extended by a decanter model which considers two liquid phases.

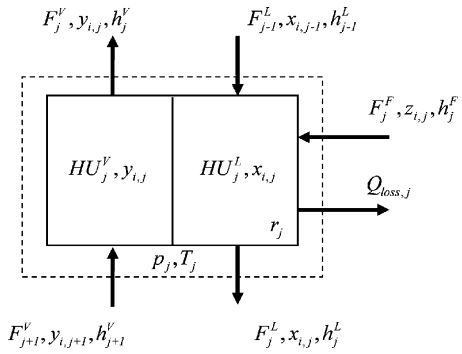

Fig. 1. Schematic diagram of an equilibrium stage (operating range model).

2.1. Operating range modelling

The simulation model for the operating range comprises for every column stage j the dynamic MESH equations (2)–(6). A schematic diagram of an equilibrium stage is depicted in Fig. 1:

$$\frac{\mathrm{d}(\mathrm{HU}_j^{\mathrm{L}} x_{i,j} + \mathrm{HU}_j^{\mathrm{V}} y_{i,j})}{\mathrm{d}t} = F_j^{\mathrm{F}} z_{i,j} + F_{j-1}^{\mathrm{L}} x_{i,j-1} + F_{j+1}^{\mathrm{V}} y_{i,j+1} - F_j^{\mathrm{L}} x_{i,j} - F_j^{\mathrm{V}} y_{i,j} + \upsilon_i r_j \tag{2}$$

$$\sum_{i=1}^{\mathrm{NC}} x_{i,j} = 1 \tag{3}$$

$$\sum_{i=1}^{\mathrm{NC}} y_{i,j} = 1 \tag{4}$$

$$\frac{\mathrm{d}(\mathrm{HU}_j^{\mathrm{L}} h_j^{\mathrm{L}} + \mathrm{HU}_j^{\mathrm{V}} h_j^{\mathrm{V}} + (mc)_{\mathrm{column}}(T_j - T_0))}{\mathrm{d}t} = F_j^{\mathrm{F}} h_j^{\mathrm{F}} + F_{j-1}^{\mathrm{L}} h_{j-1}^{\mathrm{L}} + F_{j+1}^{\mathrm{V}} h_{j+1}^{\mathrm{V}} - F_j^{\mathrm{L}} h_j^{\mathrm{L}} - F_j^{\mathrm{V}} h_j^{\mathrm{V}} - Q_{\mathrm{loss}} \tag{5}$$

$$x_{i,j} \gamma_{i,j} \varphi_{0i,j}^{\mathrm{LV}} p_{0i,j}^{\mathrm{LV}} = y_{i,j} \varphi_{i,j} p_j \quad (\text{at } T_j^{\mathrm{LV}}) \tag{6}$$

The accumulation term in the energy balance considers the molar internal enthalpies of liquid and vapour as well as the energy of the column section which is calculated from the mass and the constant heat capacity of column wall and column internals. The influence of the changing pressure on the internal energy is small compared to the other terms and is therefore not taken into account. The heat transfer resistance between the product and the column is neglected. In Eq. (6) non-idealities of the liquid phase are considered using activity coefficients calculated from the NRTL model (Table 1) [21], vapour phase association of acetic acid is taken into account by fugacity coefficients from the chemical theory according to Marek [22]. In agreement with the literature cited above [5], the formation of a second liquid phase only occurs when the liquid is subcooled in the condenser and is therefore modelled

Table 1
NRTL parameters for the calculation of activity coefficients for reaction kinetics and VLE (all from [21])

i	j	a_{ij} (cal/mol)	b_{ij} (cal/mol)	α
HOAc	PrOH	−327.52	0256.90	0.3044
HOAc	PrOAc	−410.39	1050.56	0.2970
HOAc	H_2O	−342.20	1175.72	0.2952
PrOH	PrOAc	-340.02	0111.74	0.3005
PrOH	H_2O	152.51	1866.34	0.3747
PrOAc	H_2O	-667.45	3280.60	0.2564

in the decanter only. Component vapour pressures are calculated with the Antoine equation. The stage temperature T_j equals the boiling temperature T_j^{LV} resulting from the thermodynamic equilibrium condition, Eq. (7). Hydraulic correlations are taken from Engel et al. [23] for the calculation of liquid holdup by Eq. (8) and pressure drop by Eq. (9):

$$T_j = T_j^{LV} \tag{7}$$

$$\begin{aligned} HU_j^L &= HU_{static,j}^L + HU_{dynamic,j}^L \\ &= HU_j^L(F_j^L, \Delta p_j, \rho^L, \eta^L, \sigma, \text{geometry}) \end{aligned} \tag{8}$$

$$\Delta p_j = \Delta p_j(HU_j^L, \rho^V, F_{j+1}^V, \text{geometry}) \tag{9}$$

Liquid and vapour phase are both modelled, the vapour holdup is calculated from stage volume and liquid holdup by the following equation:

$$HU_j^V = \frac{1}{v^V}\ (V_j - HU_j^L v^L) \tag{10}$$

The definition of the pressure drop is given in the following equation:

$$\Delta p_j = p_{j+1} - p_j \tag{11}$$

An activity-based pseudo-homogeneous approach for reaction kinetics is used depending on the molar holdup of H^+ protons $HU_j^{H^+}$, Eq. (12). The values for reaction rate constant k_j and chemical equilibrium constant $K_{eq,j}$ together with the corresponding temperature dependencies in Eqs. (13) and (14) have been adjusted to own experimental data from a batch reactor [6]. The enthalpy of reaction is considered implicitly via heat of formations [24–26] which are contained in the molar enthalpies of the streams:

$$r_j = HU_j^{H^+} k_j \left(a_{HOAc,j} a_{nPrOH,j} - \frac{a_{nPrOAc,j} a_{H_2O,j}}{K_{eq,j}} \right) \tag{12}$$

$$k_j = 7.699 \times 10^4\ \text{mol s}^{-1}\ \text{mol}_{H^+}^{-1} \exp\left(-\frac{37084\ \text{J mol}^{-1}}{RT_j} \right) \tag{13}$$

$$K_{eq,j} = 17.52 \exp\left(\frac{366\ \text{J mol}^{-1}}{RT_j} \right) \tag{14}$$

Table 2
Listing of equations and variables for the equilibrium stage model (operating range)

Variable	Number	Equation	Number
Molar fractions ($x_{i,j}$, $y_{i,j}$)	2NC	Component balances (2)	NC
Flow rates (F_j^L, F_j^V)	2	Summation (3), (4)	2
Holdups (HU_j^L, HU_j^V)	2	Energy balance (5)	1
Temperature (T_j)	1	Equilibrium condition (6)	NC
Boiling temperature (T_j^{LV})	1	Equality of temperatures (7)	1
Pressure (p_{j+1})	1	Liquid holdup correlation (8)	1
Pressure drop (ΔP_j)	1	Pressure drop correlation (9)	1
Reaction rate (r_j)	1	Summation of volumes (10)	1
		Pressure drop definition (11)	1
		Reaction kinetics (12)	1
Total	2NC + 9	Total	2NC + 9

Specifications (e.g. feeds), inputs from other units (e.g. stages above, below) and auxiliary correlations (e.g. for enthalpies) are not taken into account.

A listing of variables and equations for this model is given in Table 2. The partial reboiler is representing an additional separation stage; in the condenser total condensation is performed.

2.1.1. Decanter modelling

The dynamic decanter model describes the demixing of the liquid stream from the condenser F^{in}. A listing of variables and equations for this model is given in Table 3. It consists of the component balances:

$$\frac{d(HU^{DC} x_i^{DC})}{dt} = F^{in} x_i^{in} - F^I x_i^I - F^{II} x_i^{II} \tag{15}$$

the correlation for the overall composition x^{DC}, which is needed for the phase split calculation:

Table 3
Listing of equations and variables for the decanter model (operating range)

Variable	Number	Equation	Number
Molar fractions (x_i^{DC}, x_i^I, x_i^{II})	3NC	Component balances (15)	NC
Holdups (HU^{DC}, HU^I, HU^{II})	3	Calculation of overall composition (16)	NC
Phase fraction (ξ^{II})	1	Holdup summation (17)	1
Flow rates (F^I, F^{II})	2	Phase allocation (18)	1
Pressure (p^{DC})	1	Summation (19)	1
Temperature (T^{DC})	1	Outflow correlations (20), (21)	2
		Multiflash® call (22)	NC + 1
		Pressure equality (23)	1
		Temperature equality (24)	1
Total	3NC+8	Total	3NC + 8

Specifications (e.g. feeds) and inputs from other units are not taken into account.

$$\mathrm{HU}^{\mathrm{DC}} x_i^{\mathrm{DC}} = \mathrm{HU}^{\mathrm{I}} x_i^{\mathrm{I}} + \mathrm{HU}^{\mathrm{II}} x_i^{\mathrm{II}} \tag{16}$$

the holdup summation:

$$\mathrm{HU}^{\mathrm{DC}} = \mathrm{HU}^{\mathrm{I}} + \mathrm{HU}^{\mathrm{II}} \tag{17}$$

the allocation of the holdup on the two phases:

$$\mathrm{HU}^{\mathrm{II}} = \xi^{\mathrm{II}} \mathrm{HU}^{\mathrm{DC}} \tag{18}$$

and the molar fraction summation:

$$\sum_{i=1}^{\mathrm{NC}} x_i^{\mathrm{DC}} = 1 \tag{19}$$

In the experimental investigations, the liquid holdup of the two phases is controlled via valves und pumps to assure a constant level after filling up the decanter. In the model this behaviour is described by a Francis weir equation for both phases. The two weir heights $h_{\mathrm{w}}^{\mathrm{I}}$ and $h_{\mathrm{w}}^{\mathrm{II}}$ are determined from the liquid levels in the experiments:

$$F^{\mathrm{I}} = F^{\mathrm{I}}(\mathrm{HU}^{\mathrm{I}}, h_{\mathrm{w}}^{\mathrm{I}}) \tag{20}$$

$$F^{\mathrm{II}} = F^{\mathrm{II}}(\mathrm{HU}^{\mathrm{II}}, h_{\mathrm{w}}^{\mathrm{II}}) \tag{21}$$

For the phase split calculation the multiphase equilibrium package Multiflash® is used. The available functions are used to determined whether one or two liquid phases exist and to calculate the molar fractions in one liquid phase x_i^{I} and the phase fraction ξ^{II} for given temperature, pressure and overall molar composition as shown in Eq. (22). Within Multiflash® the NTRL model is applied for the liquid–liquid equilibrium (Table 4) [21,27,28]:

$$x_i^{\mathrm{I}}, \xi^{\mathrm{II}} \leftarrow \mathrm{Multiflash.TPFlash}(T^{\mathrm{DC}}, p^{\mathrm{DC}}, x^{\mathrm{DC}}) \tag{22}$$

Pressure and temperature changes in the decanter are neglected

$$p^{\mathrm{DC}} = p_{\mathrm{in}} \tag{23}$$

$$T^{\mathrm{DC}} = T_{\mathrm{in}} \tag{24}$$

Both liquid outflows can be split into a distillate and a reflux stream.

2.2. Startup modelling

The considered startup of a RD column begins when feed is entering the cold and empty column (reboiler and decanter may be charged initially). The lower part of the column is filled (the packing is wetted) until enough liquid has accumulated in the column bottom and the reboiler is switched on. When the bottom liquid starts boiling, vapour ascents in the column and heats up the bottommost section until the boiling point is reached there as well and the vapour further ascents. Since a part of vapour condenses on the cold internals, the upper part of the column is filled up as well by internal reflux. When the vapour reaches the column head it is condensed, and after a certain liquid level has built up in the decanter, the reflux is switched on. The startup is finished when product specifications are attained. This startup process is described with a modelling procedure containing the following assumptions.

Table 4
NRTL parameters for the calculation of activity coefficients for LLE

i	j	a_{ij} (cal/mol)	b_{ij} (cal/mol)	α
HOAc	PrOH	−327.52	256.90	0.3044
HOAc	PrOAc	−1971.49	1483.89	0.2000
HOAc	H_2O	1971.01	−993.17	0.2000
PrOH	PrOAc	−86.17	467.23	0.2000
PrOH	H_2O	−1102.19	2949.22	0.2000
PrOAc	H_2O	602.82	3023.94	0.2000

HOAc–PrOH: [21]; HOAc–PrOAc, HOAc–H_2O: fit to exp. data from [27,28]; others: [27].

At the beginning of startup there are no liquid or vapour streams, so that the correlations for liquid holdup and pressure drop, presented in Eqs. (8) and (9), are replaced by Eqs. (25) and (26). At low temperatures T_j the equilibrium relation in Eq. (6) does not hold because the conditions are far from boiling state. The pressure p_j is therefore not equal to the sum of the component's partial pressures but set to a constant initial value, Eq. (27). The temperature results from the energy balance and is independent from thermodynamic equilibrium ($T_j \neq T_j^{\mathrm{LV}}$, Eq. (7) is deleted). The vapour phase is not considered, Eq. (10) is replaced by Eq. (28):

$$F_j^{\mathrm{L}} = 0 \tag{25}$$

$$F_{j+1}^{\mathrm{V}} = 0 \tag{26}$$

$$p_j = p_{\mathrm{initial}} \tag{27}$$

$$\mathrm{HU}_j^{\mathrm{V}} = 0 \tag{28}$$

Three switching points are necessary for each column stage to obtain the operating point model (Eqs. (2)–(14)) from the equation set at the beginning of startup (with Eqs. (25)–(28) replacing Eqs. (7)–(10)). With every set of equations the same variables (as listed in Table 2) are calculated, the number of equations is not affected by the switching. The conditions for the switching can be reached in different order, depending on the position of the column stage relative to the feed. When liquid enters a stage, the packing is wetted until the holdup is higher than the static holdup. At that time liquid leaves this stage and the liquid holdup correlation is integrated in the model as shown in the following equation:

$$\text{if} \quad \mathrm{HU}_j^{\mathrm{L}} > \mathrm{HU}_{\mathrm{static},j}^{\mathrm{L}} \quad \text{then Eq. (25)} \rightarrow \text{Eq. (8)} \tag{29}$$

When the pressure below the considered stage p_{j+1} is higher than the stage pressure p_j, vapour is entering this stage as described by the pressure drop correlation:

$$\text{if } p_{j+1} > p_j \quad \text{then Eq. (26)} \rightarrow \text{Eq. (9)} \tag{30}$$

The temperature on a stage will increase due to the inflow of hot feed or vapour or due to a heat flux (in case of the reboiler). When the stage temperature T_j reaches the boiling point T_j^{LV}, pressure and temperature are coupled via the equilibrium equation and the vapour phase is integrated in the model. Before this point all entering vapour is assumed to condense.

if $T_j \geq T_j^{LV}(p_{initial}, x_{i,j})$ then Eq. (27) → Eq. (7),

then Eq. (28) → Eq. (10) (31)

In the decanter model the possible formation of a second liquid phase is considered during the whole startup with the Multiflash® functions in Eq. (22). Liquid outflow is zero for both phases until the respective weir height is reached.

3. Experimental investigations

Reactive distillation experiments have been carried out in an 80 mm glass column containing three reactive sections and one rectifying section at the top, each with a height of 1 m (Fig. 2). The reactive sections are packed with 8 mm × 8 mm Raschig rings and the rectifying section with Sulzer CY packing (both with a HETP of 0.2 m). The reboiler with a liquid holdup of approximately 10 l is heated by an oil-boiler (maximum heating power 3 kW) and insulated with mineral wool whereas the column is equipped with two heating jackets in order to minimize heat losses. Acetic acid is fed to the column together with the catalyst sulphuric acid below the rectifying section (preheated to 65 °C) and propanol is fed to the column bottom (preheated to 71 °C). The distillate is collected in a decanter operated at ambient pressure. Temperatures are measured at five positions in the column, in the feed streams and in the decanter (measurement error <1 °C). Samples are taken from the reboiler and both phases in the decanter. All samples are analysed by gas chromatography (Varian 3800) using a cross-linked polyethylene glycol CP-WAX 52 CB 30 m × 0.32 mm column with FID detector. Additionally for measuring the quantity of water a Karl–Fischer titration has been performed (METTLER DL 35). In case of the reboiler, the samples have been taken from the vapour phase to avoid the introduction of sulphuric acid to the gas chromatograph. Liquid composition values for comparison

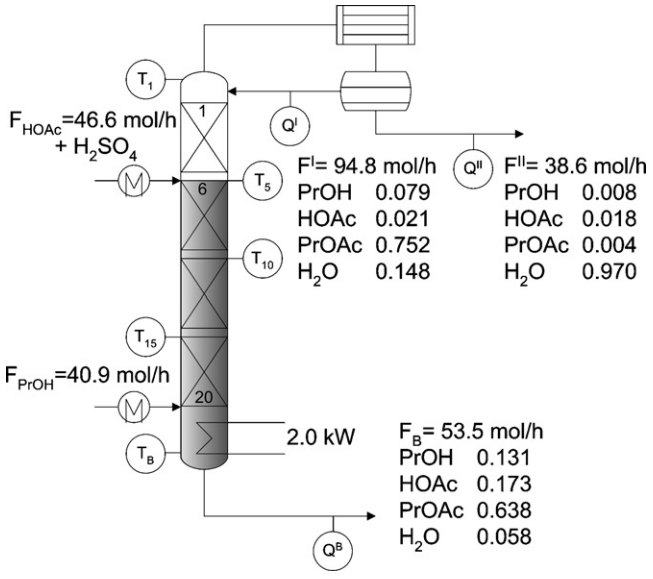

Fig. 2. Setup of RD pilot plant with experimental results (compositions in molar fractions).

Table 5
Specifications of the simulation

Pressure (bar)	1.013
Number of theoretical plates	20
Stage of HOAc feed	6
Stage of PrOH feed	20
Heat duty reboiler (kW)	2.0
Heat loss column (W)	0
Reboiler volume (l)	10
Decanter volume (l)	3.5
Diameter (mm)	80
Total packed height (m)	4
HETP Raschig, CY (m)	0.2

with the simulation have been calculated with the VLE model. Measurement errors for the molar fractions have been evaluated to be in the range of 5% [29].

The dynamic experimental results from a typical run (see Table 5 and Fig. 2 for the setup) have been used for validation of the complete model including the startup. Reboiler and decanter were empty at the beginning and were filled during startup with feed or distillate, respectively and the levels were afterwards held constant. The whole organic phase was refluxed to the column whereas the whole aqueous phase was withdrawn from the process. Reboiler duty was increased from 0 to 2 kW following a ramp during the first 1.5 h of startup. The measured temperatures in the reboiler (T_B) and at the column top (T_1) are compared with the simulation results in Fig. 3. Very good agreement of both dynamic and stationary values is reached; the time until vapour reaches the top is correctly predicted. Since the first rising vapour does not meet any liquid counter current above the upper feed, the acetic acid fraction is temporarily rising in the top of the column leading to higher temperatures T_1 than T_B until the reflux is turned on. In Figs. 4 and 5 a comparison of the simulated dynamic composition trends in the decanter (organic phase) and the reboiler with the compositions from the analysis of the samples that have been taken during the whole experimental run is depicted. The time axis on the diagram starts when the first samples are taken, after filling up the vessels. The dynamic behaviour is reproduced very well by the simulation for both reboiler and decanter. In case of the heavy phase composition, which is not shown, the high water fraction is reached after a very

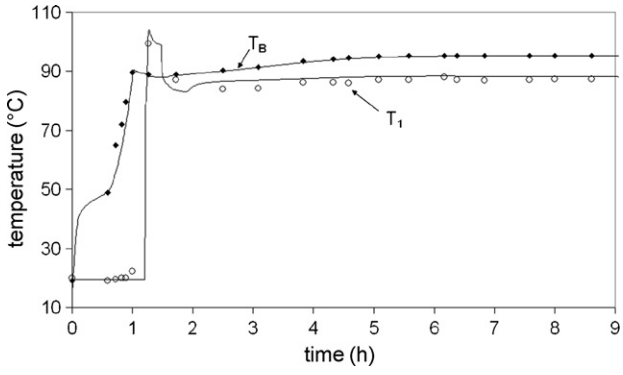

Fig. 3. Dynamic temperature trend in column bottom (T_B) and column head (T_1) from experiment and simulations.

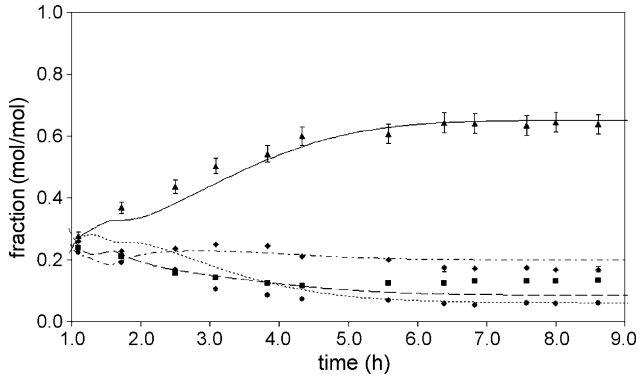

Fig. 4. Dynamic composition trend in the reboiler (liquid phase) from experiment (PrOH (■); HOAc (♦); PrOAc (▲); H_2O (●)) and simulation (PrOH, dashed line; HOAc, dash-dot line; PrOAc, solid line; H_2O, dotted line) during column startup. Experimental values calculated from measured vapour phase composition assuming phase equilibrium. Error bars (5%) can only be depicted for PrOAc.

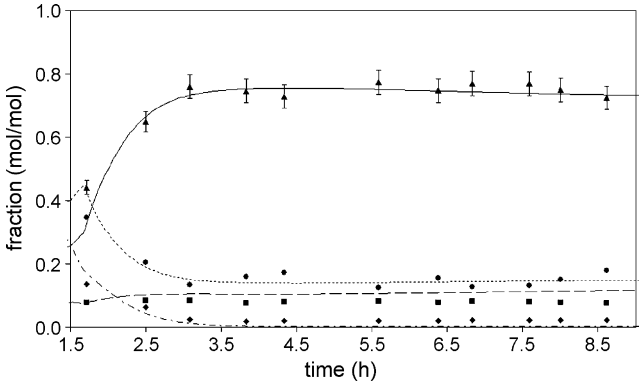

Fig. 5. Dynamic composition trend of the organic phase in the decanter from experiment (PrOH (■); HOAc (♦); PrOAc (▲); H_2O (●)) and simulation (PrOH, dashed line; HOAc, dash-dot line; PrOAc, solid line; H_2O, dotted line) during column startup. Error bars (5%) can only be depicted for PrOAc.

Table 6
Experimental measurements of the temperature in column bottom and column top

Time (h)	T_B (°C)	T_1 (°C)
0.00	20.0	19.9
0.58	48.9	19.1
0.72	65.0	19.5
0.82	72.0	20.0
0.88	79.6	20.0
1.00	89.7	22.2
1.27	88.9	99.3
1.72	89.0	87.2
2.50	90.3	84.0
3.08	91.5	84.2
3.83	93.4	86.2
4.33	94.2	86.3
4.58	94.6	86.1
5.08	95.1	87.1
5.58	95.3	87.1
6.17	95.2	88.1
6.38	95.3	87.1
6.83	95.2	86.9
7.58	95.3	87.2
8.00	95.2	87.3
8.62	95.2	87.4

short time in both simulation and experiment. The experimental values corresponding to Figs. 3–5 are given in Tables 6 and 7.

4. Analysis of the startup

For the analysis of the startup of the RD process for propyl acetate production, two different designs with 25 column sections each have been considered, providing higher product purity compared to the experimental configuration (approximately 85% of PrOAc). Thus, it is possible to compare the startup behaviour of two different RD processes designed for the same objective. In case of design A the product rich in PrOAc is with-

Table 7
Experimental values of molar compositions in column bottom (liquid phase, calculated from measured vapour phase composition assuming phase equilibrium) and both liquid phases in the decanter

	Time											
	1.10 h	1.72 h	2.50 h	3.08 h	3.83 h	4.33 h	5.58 h	6.38 h	6.83 h	7.58 h	8.00 h	8.62 h
Bottom composition (mol/mol)												
PrOH	0.238	0.210	0.158	0.142	0.126	0.115	0.124	0.124	0.132	0.131	0.131	0.134
HOAc	0.261	0.229	0.237	0.248	0.245	0.210	0.199	0.174	0.172	0.174	0.167	0.167
PrOAc	0.277	0.369	0.436	0.504	0.543	0.601	0.607	0.644	0.641	0.635	0.644	0.638
H_2O	0.224	0.192	0.168	0.106	0.087	0.074	0.069	0.059	0.054	0.060	0.057	0.061
Decanter, organic phase composition (mol/mol)												
PrOH		0.078	0.083	0.083	0.075	0.079	0.082	0.078	0.081	0.080	0.078	0.076
HOAc		0.135	0.063	0.025	0.018	0.020	0.020	0.020	0.021	0.021	0.021	0.021
PrOAc		0.442	0.649	0.760	0.747	0.730	0.773	0.748	0.771	0.769	0.750	0.725
H_2O		0.346	0.204	0.133	0.160	0.171	0.125	0.154	0.127	0.130	0.152	0.178
Decanter, aqueous phase composition (mol/mol)												
PrOH		0.014	0.011	0.010	0.008	0.012	0.006	0.008	0.008	0.008	0.008	0.008
HOAc		0.048	0.016	0.007	0.006	0.013	0.010	0.019	0.017	0.017	0.017	0.018
PrOAc		0.008	0.004	0.004	0.004	0.005	0.003	0.004	0.004	0.004	0.004	0.004
H_2O		0.930	0.968	0.979	0.981	0.970	0.980	0.969	0.971	0.970	0.971	0.970

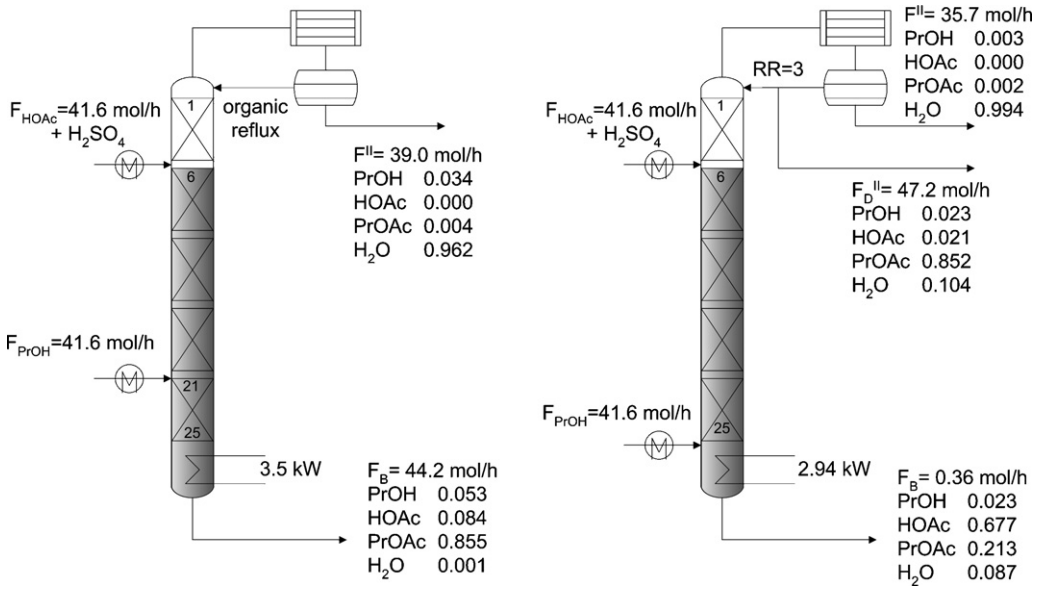

Fig. 6. Design A (left) and B (right) of the RD column for the startup simulations (compositions in molar fractions).

drawn from the column bottom and the complete organic phase forms the reflux, whereas for design B the product is taken from the organic phase in the decanter (Fig. 6). In both designs the aqueous phase is withdrawn from the process in the decanter. To avoid accumulation of non-reacted acetic acid in the column a small purge from the bottom is necessary for design B which could be recycled with the acetic acid feed (not shown in figure). The other specifications (diameter, packing type, reboiler and decanter volume) are the same as given in Section 3 (Table 5). The resulting composition profiles for the operating point in the columns are shown in Fig. 7. The profiles are very different for the two designs; especially the acetic acid fraction is much higher in design B throughout the whole column. In both cases this column is part of a complete process containing at least one additional separation step to gain pure acetate. Here only the RD column is considered. Further considerations of design issues can be found in Ref. [6].

With the experimentally validated model, simulation studies are carried out to compare different startup policies. Since, Reepmeyer et al. [11] and Forner et al. [12] have shown the strong influence of initial charging of column or vessels on the startup time of reactive distillation processes, the effect of initial charging of reboiler and decanter is analysed for both designs. The considered initial compositions are pure educts or products and steady-state compositions; the initial temperature is always 25 °C. The flow rate of the preheated feed and the reboiler duty are always fixed to their corresponding steady-state values during startup. The measure for reaching steady state is the MX-

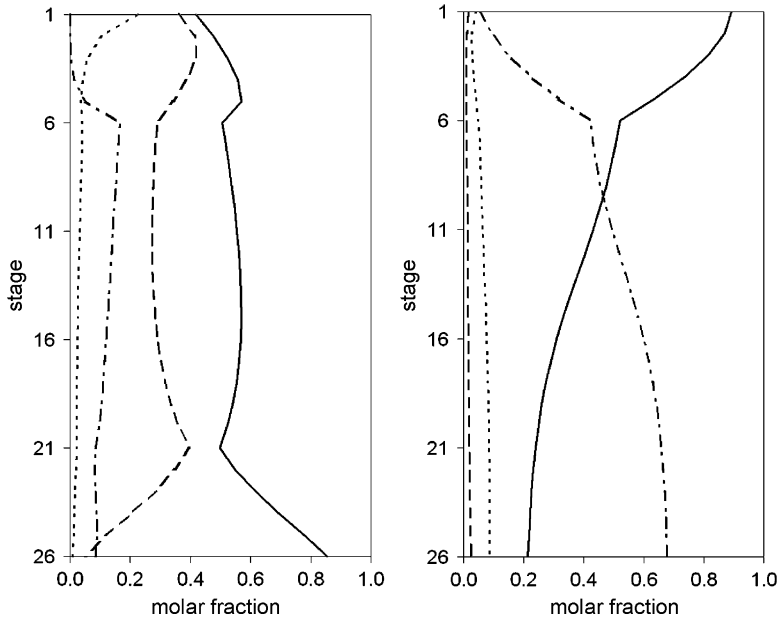

Fig. 7. Composition profiles in the RD column for design A (left) and design B (right): PrOH, dashed line; HOAc, dash-dot line; PrOAc, solid line; H_2O, dotted line.

Table 8
Initial compositions and startup time for the different simulation runs (steady-state if MX < 0.01)

	Initial charging reboiler	Initial charging decanter	Steady-state bottom	Steady-state top	Steady-state all
Design A					
Case A1	Empty	Empty	448 min	151 min	656 min
Case A2	Steady state	Steady state	−41%	−52%	−28%
Case A3	Empty	HOAc	33%	25%	23%
Case A4	PrOAc	Steady state	−66%	−69%	−45%
Design B					
Case A1	Empty	Empty	6330 min	4740 min	8840 min
Case A2	Steady state	Steady state	−69%	−91%	−36%
Case A3	HOAc	Steady state	−92%	−88%	−56%
Case A4	HOAc	HOAc	−92%	−88%	−56%

The time needed to fill up the reboiler and the decanter has been subtracted from the base case startup time. For cases 2–4, the difference to case 1 is given.

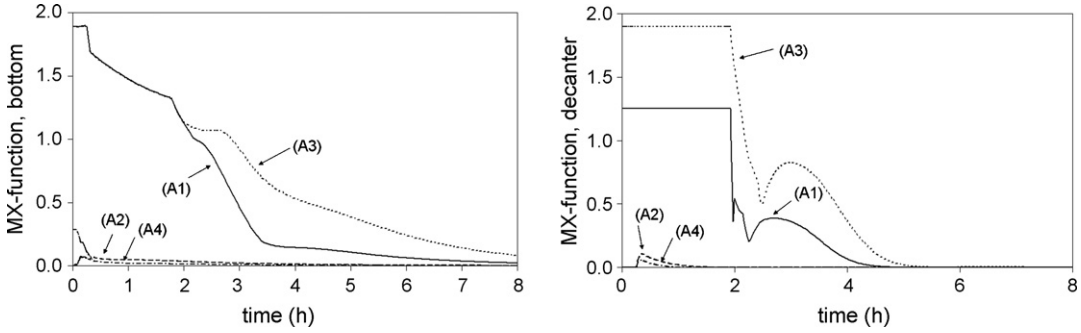

Fig. 8. MX-function at bottom (left) and top (right) for design A: case A1, solid line; case A2, dashed line; case A3, dotted line; case A4, dash-dot line.

function in Eq. (32), presented by Yasuoka and Nakanishi [30]:

$$MX = \sum_{i}^{NC} |x_i^{\text{current}} - x_i^{\text{steady state}}| \tag{32}$$

This function gives the sum of deviations between the current composition and the steady-state composition over all components. If the MX-function is permanently below a certain bound which is set to 0.01 in these studies, the desired steady state is defined to be reached. The MX-function is calculated for the organic phase in the decanter (MX top) and the bottom composition (MX bottom) as well as for the whole column (MX all, summation over all stages).

For both designs the simulated startup time for the base case (case A1/B1, initially empty vessels) is listed in Table 8. The time that is needed during startup to fill the column bottom (design A, 110 min; B, 109 min) and the decanter (design A, 9 min; B, 11 min) is not included in the base case startup time for better comparison with the startup times of the alternative strategies. For three exemplary cases each (cases A2–A4 and B2–B4) the reduction or extension of startup time compared to the base case is listed as well in Table 8. The great influence of the initial charging is shown. In case of design A charging pure PrOAc to the reboiler and product with steady-state composition to the decanter (A4) leads to a reduction of startup time of 66% (considering the bottom MX-function) or 45% until the whole column has reached the steady state. This behaviour is illustrated in the trends of the MX-functions in Fig. 8. Only the product MX-functions which give the time until the desired product specification is reached are depicted. For cases A2 and A4 with initial top and bottom compositions close to the steady state, the value of the MX-function is always close to zero, neither the feed entering the reboiler nor the first distillate arriving at the decanter leads to a large disturbance. In contrast initial charg-

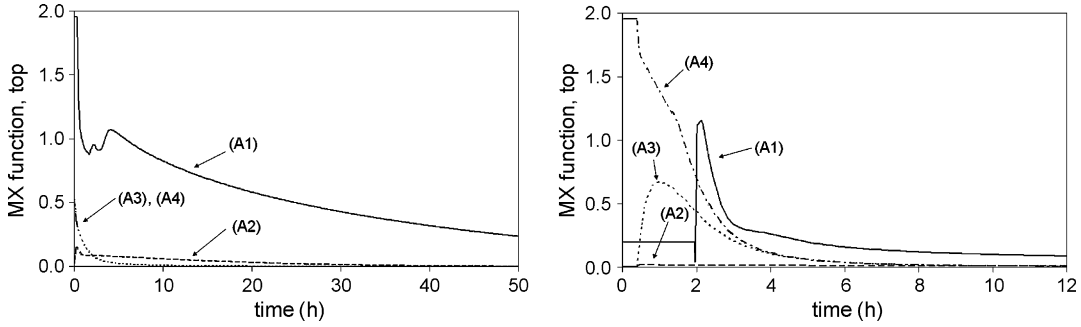

Fig. 9. MX-function at bottom (left) and top (right) for design B: case B1, solid line; case B2, dashed line; case B3, dotted line; case B4, dash-dot line.

ing of acetic acid to the decanter together with an initially empty reboiler (case A3) extends the startup time by 33% (bottom).

For design B much longer startup times are calculated. This can be explained with the need to purge the non-reacted acetic acid from the column bottom. For this purpose rather high acetic acid fractions in the bottom (67.7%) have to be established by accumulation which takes a longer time as shown in Fig. 9(left) for case B1 (startup with empty vessels). Charging product with a high acetic acid fraction to the reboiler can therefore dramatically reduce the startup time (cases B2–B4). The top product composition reaches steady state fastest by initial charging of product with steady-state compositions to column bottom and decanter (91% reduction in case B2). Due to the dominating influence of the bottom composition the startup time for the whole column is shortest when pure acetic acid is charged to the reboiler (56% reduction in cases B3 and B4). The phenomenon described by Tran [10] that charging of product with steady-state composition to the decanter can increase startup time is not observed for the considered process. The occurrence of multiple steady states in the system investigated by Tran [10] could be an explanation for these deviant findings.

5. Conclusion

A simulation model for the startup of reactive distillation in packed columns for systems with two liquid phases has been presented. The results of a validation of this model with experimental data for the esterification of propanol with acetic acid show that the dynamic behaviour of the process during the whole startup period starting from cold and empty state is well described. Simulation studies for this process have been carried out which demonstrate the great influence of initial charging of reboiler and decanter on the startup of a packed column. The slight deviations in the simulation results compared to our earlier publication at SIMO'06 [31] are due to a modification of the kinetic parameters after adjustment to additional experimental data [6]. The conclusions which are drawn from our studies are not affected. The two considered designs show very different startup behaviour. For both, significant reduction of startup time up to 66% (design A) and 91% (design B) until the product meets the specifications can be reached for the considered process leading to considerably lower operating costs. On the basis of the results of these simulation studies mathematical optimisation is currently carried out to determine the optimal initial conditions for the startup.

Acknowledgement

The authors gratefully acknowledge the financial support from the DAAD through the PROCOPE program.

Appendix A. Nomenclature

a	specific surface (m^2/m^3)
a_i	activity
c	heat capacity (J/(mol K))
F	flow rate (mol/s)
h	molar enthalpy (J/mol)
h_W	weir height (m)
HU	molar holdup (mol)
$HU^L_{dynamic}$	dynamic liquid holdup (mol)
HU^L_{static}	static liquid holdup (mol)
k	reaction rate constant (mol/s)
K_{eq}	chemical equilibrium constant
m	mass (kg)
NC	number of components
p	pressure (bar)
Δp	pressure drop (bar)
$p_{initial}$	initial pressure (bar)
p^{LV}_{0i}	component i vapour pressure (bar)
Q_{loss}	heat loss (W)
r	reaction rate (mol/s)
R	ideal gas constant (J/(mol K))
RR	reflux ratio
T	temperature (K)
T_0	reference temperature (K)
T_{LV}	boiling temperature (K)
v	molar volume (m^3/mol)
V	volume (m^3)
x	molar fraction, liquid (mol/mol)
y	molar fraction, vapour (mol/mol)
z	molar fraction, feed (mol/mol)

Greek symbols

ε	void fraction
φ^{LV}_{0i}	fugacity coefficient of pure component i at its vapour pressure and system temperature
φ_i	fugacity coefficient of component i in the mixture at system temperature and pressure
γ_i	activity coefficient
η	dynamic viscosity (kg/(m s))
ξ	phase fraction
ρ	density (kg/m^3)
σ	surface tension (N/m)
υ_i	stoichiometric coefficient

Subscripts

B	bottom
D	distillate
i	component
j	column stage

Superscripts

DC	decanter
F	feed
H^+	referring to H^+ protons
I	first liquid phase (organic)
II	second liquid phase (aqueous)
in	incoming
L	liquid
V	vapour

References

[1] V.H. Agreda, L.R. Partin, Reactive distillation process for the production of methyl acetate, United States Patent 4,435,595 (1984).

[2] M.M. Sharma, S.M. Mahajani, in: K. Sundmacher, A. Kienle (Eds.), Reactive Distillation, Wiley-VCH, Weinheim, 2003, ISBN 3-527-30579-3, pp. 3–29.

[3] Y.-T. Tang, Y.-W. Chen, H.-P. Huang, C.-C. Yu, S.-B. Hung, M.-J. Lee, Design of reactive distillations for acetic acid esterification, AIChE J. 51 (2005) 1683–1699.

[4] A. Singh, R. Hiwale, S.M. Mahajani, R.D. Gudi, J. Gangadwala, A. Kienle, Production of butyl acetate by catalytic distillation, theoretical and experimental studies, Ind. Eng. Chem. Res. 44 (2005) 3042–3052.

[5] R. Khaledi, P.R. Bishnoi, A method for modeling two- and three-phase reactive distillation columns, Ind. Eng. Chem. Res. 45 (2006) 6007–6020.

[6] M. Brehelin, F. Forner, D. Rouzineau, J.-U. Repke, X. Meyer, M. Meyer, G. Wozny, Production of *n*-propyl acetate by reactive distillation: experimental and theoretical study, Chem. Eng. Res. Des. 85 (2007) 109–117.

[7] H.Z. Kister, Distillation Operation, McGraw Hill, New York, 1990, ISBN 007034910X.

[8] M. Flender, Zeitoptimale Strategien für Anfahr- und Produktwechselvorgänge an Rektifizieranlagen, Dissertation, Technische Universität Berlin, VDI Verlag, Düsseldorf, 1999, ISBN 3-18-361003-5.

[9] K. Löwe, G. Wozny, Development and experimental verification of a time-optimal startup strategy for a high purity distillation column, Chem. Eng. Technol. 23 (2000) 841–845.

[10] T.K. Tran, Analyse des Anfahrens von Dreiphasenkolonnen, Dissertation, Technische Universität Berlin, Shaker Verlag, Aachen, 2005, ISBN 3-8322-2623-6.

[11] F. Reepmeyer, J.-U. Repke, G. Wozny, Time optimal start-up strategies for reactive distillation columns, Chem. Eng. Sci. 59 (2004) 4339–4347.

[12] F. Forner, M. Döker, J. Gmehling, J.-U. Repke, G. Wozny, Anfahrstrategien für die Reaktivrektifikation in Boden- und Packungskolonnen, Chem. Ing. Tech. 79 (2007) 367–376.

[13] N. Scenna, C. Ruiz, S. Benz, Dynamic simulation of start-up procedures of reactive distillation columns, Comput. Chem. Eng. 22 (1998) 719–722.

[14] N.J. Scenna, S.J. Benz, Start-up operation of reactive columns with multiple steady states: the ethylene glycol case, Ind. Eng. Chem. Res. 42 (2003) 873–882.

[15] H.-X. Wu, Z.-G. Tang, H.-B. Gao, H. Hu, X.-C. Lu, S.-Y. Li, Effects of liquid holdup in condensers on the start-up of reactive distillation columns, Chem. Eng. Technol. 29 (2006) 1316–1322.

[16] R. Taylor, R. Krishna, Modelling reactive distillation, Chem. Eng. Sci. 55 (2000) 5183–5229.

[17] S. Steinigeweg, Zur Entwicklung von Reaktivrektifikationsprozessen am Beispiel gleichgewichtslimitierter Reaktionen, Dissertation, Carl von Ossietzky Universität Oldenburg, Shaker Verlag, Aachen, 2003, ISBN 3-8322-2104-2.

[18] T. Pöpken, Reaktive Rektifikation unter besonderer Berücksichtigung der Reaktionskinetik am Beispiel von Veresterungsreaktionen, Dissertation, Carl von Ossietzky Universität Oldenburg, Shaker Verlag, Aachen, 2005, ISBN: 3-8265-8638-7.

[19] P. Moritz, S. Blagov, H. Hasse, Heterogen katalysierte Reaktivdestillation: Design und Scale-up am Beispiel von Methylacetat, Chem. Ing. Tech. 74 (2002) 1207–1218.

[20] C.A. Ruiz, I.T. Cameron, R. Gani, A generalized dynamic model for distillation columns. III. Study of startup operations, Comp. Chem. Eng. 12 (1988) 1–14.

[21] J. Gmehling, U. Onken, Vapour–liquid equilibrium data collection, Chemistry Data Series, DECHEMA, Frankfurt am Main, 1977.

[22] J. Marek, Vapor–liquid equilibria in mixtures containing an associating substance. II. Binary mixtures of acetic acid at atmospheric pressure, Collect. Czech. Chem. Commun. 20 (1955) 1490–1502.

[23] V. Engel, J. Stichlmair, W. Geipel, Fluid dynamics of packings for gas–liquid contactors, Chem. Eng. Technol. 24 (2001) 459–462.

[24] J.A. Riddick, W.A. Bunger, T.S. Sakano, Organic Solvents Physical Properties and Methods of Purification, 4th ed., Wiley, New York, 1986, ISBN 0-471-08467-0.

[25] I. Barin, Thermochemical Data of Pure Substances, 3rd ed., Wiley-VCH, Weinheim, 1995, ISBN 3-527-28745-0.

[26] E.S. Domalski, E.D. Hearing, Estimation of the thermodynamic properties of C–H–N–O–S–halogen compounds at 298.15 K, J. Phys. Chem. Ref. Data 22 (1993) 805–1159.

[27] W. Arlt, M.E.A. Macedo, P. Rasmussen, J.M. Sorensen, Liquid–liquid equilibrium data collection, Chemistry Data Series, DECHEMA, Frankfurt am Main, 1979.

[28] X. Xiao, L. Wang, G. Ding, X. Li, Liquid–liquid equilibria for the ternary system water + acetic acid + propyl acetate, J. Chem. Eng. Data 51 (2006) 582–583.

[29] M. Brehelin, Analyse de faisabilité, conception et simulation de la distillation réactive liquide-liquide-vapeur. Application et validation expérimentale sur la production de l'acétate de *n*-propyle, Dissertation, ENSIACET, Toulouse, 2006.

[30] H. Yasuoka, E. Nakanishi, Design of an on-line startup system for a distillation column based on a simple algorithm, Int. Chem. Eng. 27 (1987) 466–472.

[31] F. Forner, M. Brehelin, D. Rouzineau, M. Meyer, J.-U. Repke, Startup of a Reactive Distillation Process with a Decanter—Simulation and Experimental Validation, SIMO, Toulouse, 2006.